ALTERNATIVE DESIGN FOR THE RISP PRE-STRIPPER LINAC*

B. Mustapha†, P.N. Ostroumov, Z.A. Conway, M.P. Kelly, and A. Plastun,
Argonne National Laboratory, Lemont, IL, USA,
J.-H. Jang, H. Jin, J.-W. Kim and H.J. Kim, RISP, IBS, Korea

Abstract

In a collaborative effort between Argonne's Linac Development Group and the RISP project team at the Korean Institute for Basic Science, we have developed an alternative design for the pre-stripper section of the RISP driver linac. The proposed linac design takes advantage of the recent accelerator developments at Argonne, namely the ATLAS upgrades and the Fermilab PIP-II HWR Cryomodule. In particular, the state-of-the-art performance of QWRs and HWRs, the integrated steering correctors and clean BPMs for a compact cryomodule design. To simplify the design and avoid frequency transitions, we used two types of QWRs at 81.25 MHz. The QWRs were optimized for β ~ 0.05 and ~ 0.11 respectively. Nine cryomodules are required to reach the stripping energy of 18.5 MeV/u. Following the lattice design optimization, end-to-end beam dynamics simulations including most important sources of machine error were performed. The results showed that the design is tolerant to errors with no beam losses observed for nominal errors.

INTRODUCTION

The baseline design for the RISP pre-stripper linac [1], named SCL3, uses QWRs and HWRs with room-temperature quadrupole focusing between cryostats containing one or two cavities. In this alternative design, we propose long cryomodules containing 7 or 8 cavities each with SC solenoid focusing. This design has the potential of significantly reducing the length and construction cost of the linac while satisfying the same beam requirements.

QWR CHOICE & EM DESIGN

Based on the frequency and the velocity range of the RISP pre-stripper linac, QWR type cavities are an ideal match for this section. In addition, using only QWRs will avoid a frequency transition in the middle of the linac if HWRs are used. At ANL, we have successfully developed and operated QWR resonators in the same frequency and velocity ranges as the ones required for the RISP pre-stripper linac [2]. Therefore, the design and fabrication of the RISP QWRs will require little to no R&D.

Two QWR types are required for the RISP pre-stripper linac, a low-β and a high-β, with β ~ 0.05 and 0.11, respectively. Both cavities are designed for 81.25 MHz frequency with 40 mm diameter aperture. The EM design of the two QWRs was performed based on the design optimization procedure developed at ANL [3]. The main RF parameters, such as the shunt impedance and peak fields, were optimized by varying the geometry parameters of the cavities. The proposed geometries have tapered inner and outer conductors spreading the magnetic field over a larger area which helps reduce the peak surface magnetic field. It is important to note that tapering the outer conductor does not add to the real-estate of the linac but uses the available space between elements.

Table 1 lists the RF parameters of the optimized designs for both QWRs while the geometry and the EM field distributions are shown in Figure 1.

Table 1: RF Design Parameters of the Two QWRs

Parameter	Low-β	High-β
β_{opt}	0.05	0.11
L_{eff}	18.5	40.5
E_{peak}/E_{acc}	5.6	5.6
B_{peak}/E_{acc}	7.7	7.3
R/Q (Ω)	493	552
G (Ω)	23	32

Following the design optimization of the cavities, the EM fields were extracted and used for beam simulations of the linac. This step is important to study the beam steering effects expected from these QWRs and apply the steering corrections by tilting the faces of the drift tubes. For the low-β, the required angle is 1 deg, while it is 4 deg for the high-β QWR.

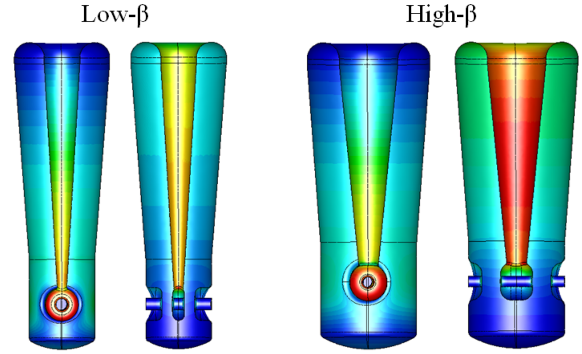

Figure 1: Geometries and EM field distributions for both types of QWRs.

LINAC LATTICE DESIGN

Ion beam acceleration from 500 keV/u to 18.5 MeV/u requires 2 types of QWRs as discussed in the

* This work was supported by the work-for-other grant WFO8550H titled "Pre-conceptual design, cost and schedule estimate of the 18.5 MeV/u Pre-stripper linac for the RISP/IBS.
†corresponding author: brahim@anl.gov

ISBN 978-3-95450-169-4

previous section. We propose to build 2 cryomodules of low-beta QWRs and 7 cryomodules of high-beta QWRs. The layouts for the different types of cryomodule are shown in Figure 2. The voltage is slowly ramped in the first cryomodule to better control the longitudinal motion and a SC solenoid is placed after each of the first two cavities to better control the transverse motion of the beam. Hence, the highest accelerating field for the first several cavities is limited by the non-linearity of the particle motion not by any fundamental cavity limit. In the second low-β cryomodule, we can use an additional SC cavity instead of the second solenoid. In this way, the mechanical design of the cryomodules is the same while an extra SC cavity will be available to provide better operational reliability of the system. The high-beta cryomodule has a more standard two-cavity one-solenoid structure operating at the full design voltage.

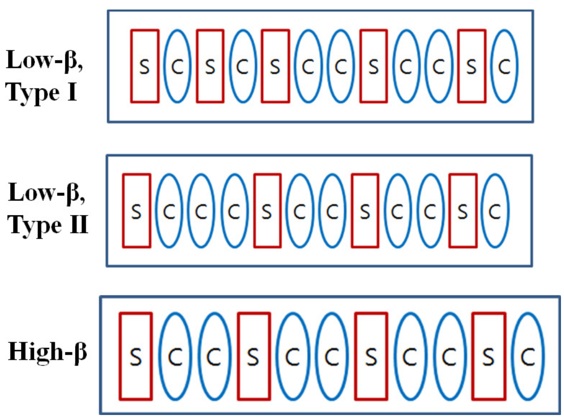

Figure 2: Layouts of the different types of cryomodule.

The layout of the proposed RISP cryomodules is very similar to the ATLAS intensity upgrade and PIP-II cryomodules [2, 4]. The lattice includes extra space between cryomodules for diagnostics, pumping connections and other applications. The inter-module distance could be adjusted in the future with minimal effect on the beam dynamics.

BEAM DYNAMICS DESIGN

The goals of the beam dynamics design and simulations are (1) to provide matching between the RFQ and the SC linac, (2) to define the value of the accelerating voltage and synchronous phase for each SC cavity and the solenoid field and (3) to demonstrate zero-loss beam acceleration in the pre-stripper linac. The simulation starts from the multi-harmonic buncher (MHB) with a dual charge state uranium beam (33+ and 34+). To define the parameters of the accelerating and focusing lattice, a relatively low number of particles is used, typically 10^4 for each charge state of uranium. The space charge effects for uranium beam are negligible after the RFQ. The criteria for the linac parameters selection is the proper matching in the longitudinal and transverse phase space for each focusing period along the linac. In particular, good matching must be provided in the transitions between cryomodules. The available voltage from the SC resonators in the first two cryomodules exceeds the limit dictated by a smooth and adiabatic acceleration and can introduce significant non-linear motion in the longitudinal phase space if fully used. Therefore, we have applied ramping of both the accelerating voltage and synchronous phase in the first two cryomodules. Similarly, the strengths of the SC solenoids were optimized to produce a smooth transverse phase advance along the linac.

Figure 3 shows a TRACK screenshot for the simulation of a uranium beam from the MHB to the end of the pre-stripper linac. This simulation used 500k particles in each charge state (33+ and 34+) where 98.83% particles are accepted by the RFQ and accelerated in the linac with no beam loss. We have also studied the proton beam dynamics. Protons can be accelerated up to 80 MeV in this linac. Despite the higher voltages per nucleon applied in the SC cavities, no active transverse steering is required for the proton beam without machine errors. This fact indicates that the steering compensation in the SC cavities works very well.

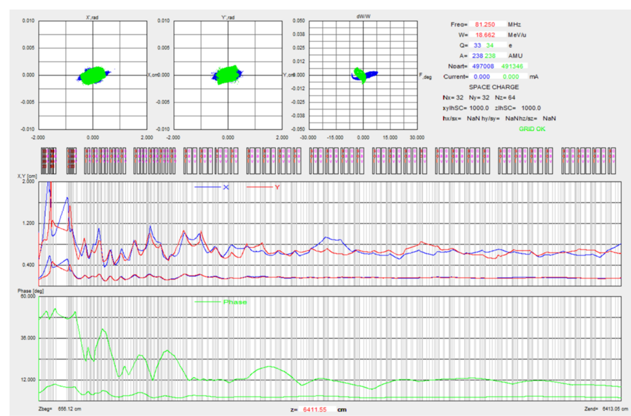

Figure 3: TRACK beam dynamics for a dual charge state uranium beam (33+ and 34+) along the linac.

MACHINE ERROR SIMULATIONS

We have performed beam simulations for the SC linac including different sources of machine error. Three sets of error with increasing amplitudes were simulated for a two-charge state uranium beam (33+ and 34+). Table 2 lists the error types and values for every set of errors. The RF errors are jitter or dynamic errors that cannot be corrected for. The first set of error represents the nominal error values, the rf errors were doubled in the second set, while the misalignment errors were doubled in the third one. For every error set, 100 randomly generated linac configurations (also known as seeds) were simulated, each with a total of 10^5 macro-particles starting from the LEBT (50 k for each charge state). Both cases, before and after applying corrective steering, were simulated to study the effect of corrections and determine the required number, location and strengths of the steering coils.

Table 2: Error types and amplitudes for three sets of errors used in the simulations. Misalignment errors are uniform within the given maximum value and rf errors are Gaussian with given sigma value truncated at 3*sigma.

Error Set	Cav. & Sol. Misalign. (mm)	RF phase error (deg)	RF amplitude error (%)
1	0.25	0.5	0.5
2	0.25	1.0	1.0
3	0.5	0.5	0.5

The transverse correction scheme used in the error simulations with corrective steering is shown in figure 4. In this scheme, every cryomodule is treated as a separate correction section. The general idea is to use the steering coils on the solenoids placed in the middle of the cryomodule and the beam position monitors attached to the solenoid placed at the cryomodule end and between cryomodules. For every correction section, at least two monitors are required in order to correct both the position and angle of the beam. Only two correctors and two monitors are used in this scheme. In the case where the combined strength of the two central correctors is not sufficient, the third corrector placed at the cryomodule entrance can be used. In these simulations, the corrector strength was limited to 5 mrad angular kick. The monitor precision and misalignment were set to 100 microns each. With increasing error amplitudes, we expect the correction scheme to fail at one point. In this case, we can include more correctors and monitors in every correction section and or increase the correctors strength.

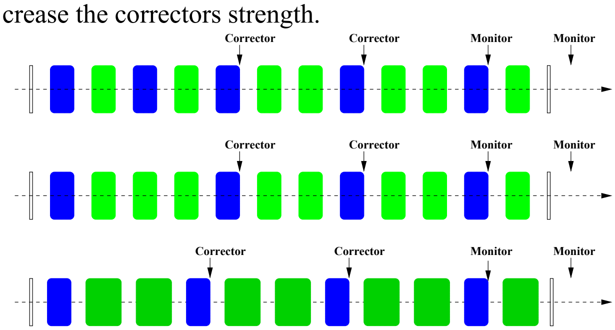

Figure 4: Correction scheme used in the error simulations. The strings correspond to the different types of cryomodule where each is treated as a separate correction section.

The results of the error simulations with and without corrective steering are shown in Figure 5 for the third set of errors with double the misalignments. On the left, the plots show the beam centroids before (in red) and after correction (in blue). On the right, they show the distribution of angular kicks and the corresponding magnetic field strength required for the corrective steering coils. It is important to note that the maximum required magnetic field integral for the corrective steering coils is 8000 Gs*cm, which would require a maximum magnetic field of 400 Gs for an effective coil length of 20 cm.

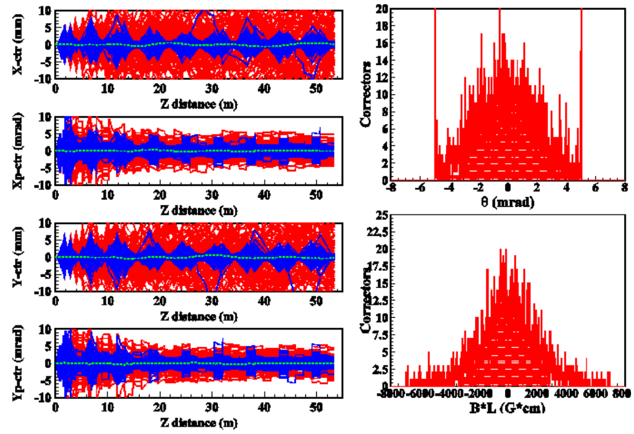

Figure 5: Error and correction simulation results for error set no.3. On the left are beam centroids before and after correction. On the right are the corrector strength in mrad and the corresponding magnetic field integral.

The beam loss fractions before and after correction for every set of errors are given in Table 3. In the case of error set no. 3, where the misalignment errors were doubled, the beam loss before corrections is significant, reaching 5% but after the correction no beam loss was observed. In the case of error set no. 2, where the rf errors were doubled, one seed produced a loss of a single macro-particle, which cannot be restored by transverse corrections. We believe that, this single macro-particle was lost longitudinally by leaving the linac acceptance before it was intercepted by an aperture. This single-particle loss measures how wide the longitudinal acceptance of the linac is, which was only reached after doubling the rf errors to 1 deg – 1% sigma values for Gaussian distributions truncated at 3 * sigma.

Table 3: Beam Loss Fraction for the Different Sets of Errors Before and After Correction

Error Set	Beam lost before correction	Beam lost after correction
1	3 10^{-7}	0
2	5 10^{-7}	1 10^{-7}
3	5%	0

Based on the results of these error and correction simulations, we can conclude that the proposed design for the RISP pre-stripper linac is robust and offer a wide range of tolerance to errors and flexibility for beam tuning without beam loss.

ISBN 978-3-95450-169-4

REFERENCES

[1] S. Jeong, "Progress of the RAON heavy ion accelerator project in Korea", in *Proceedings of IPAC-2016*, Busan, Korea, p. 4261.

[2] M.P. Kelly *et al*, "Commissioning of the 72 MHz Quarter wave Cavity Cryomodule at ATLAS", in *Proceedings of Linac-2014*, Geneva, Switzerland, p. 440.

[3] B. Mustapha *et al*, "Electro-Magnetic Optimization of a Quarter-wave Resonator", in proceedings of Linac-2010, Tsukuba, Japan, p. 169.

[4] Z. Conway *et al*, "A new 2 Kelvin Superconducting Half-Wave Cavity Cryomodule for PIP-II," IOP Conference Series: Materials Science and Engineering 101 (2015) 012019.